

# Rainfall and Dragon-Kings

O. Peters<sup>1,2,a</sup>, K. Christensen<sup>3</sup>, and J.D. Neelin<sup>4</sup>

<sup>1</sup> Dept. of Mathematics and Grantham Institute for Climate Change, Imperial College London, 180 Queens Gate, London SW7 2AZ, UK

<sup>2</sup> Dept. of Atmospheric and Oceanic Sciences, University of California, Los Angeles, 405 Hilgard Ave., Los Angeles, California 90095-1565, USA

<sup>3</sup> Dept. of Physcis, Imperial College London, Prince Consort Road, London SW7 2AZ, UK

<sup>4</sup> Dept. of Atmospheric and Oceanic Sciences, University of California, Los Angeles, 405 Hilgard Ave., Los Angeles, California 90095-1565, USA

Received 23 November 2011 / Received in final form 09 March 2012

Published online 01 May 2012

**Abstract.** Previous studies have found broad distributions, resembling power laws for different measures of the size of rainfall events. We investigate the large-event tail of these distributions and find in one measure that tropical cyclones account for a large proportion of the very largest events outside the scaling regime, *i.e.*, beyond the cutoff of the power law. Tropical cyclones are sufficiently rare that they contribute a significant number only in a regime of large event sizes that common rain events almost never reach. The different physical dynamics of tropical cyclones permits a substantial extension of the tail in this large-event regime.

## 1 Introduction

This volume addresses the re-relationship between commonly observed everyday events and uncommon extreme events in various physical systems. Are the extreme events only different by being very big (or very small) and infrequent or are they fundamentally different “Dragon-Kings”? This nomenclature was introduced by Sornette [1] to denote in particular extreme events in distributions that are well approximated by power laws in a large scaling regime. What happens outside this regime? In Ref. [1], Dragon-Kings are associated with more-likely extreme events than a simple extrapolation of the body of the distribution would suggest. In Chinese mythology, four Dragon Kings are rulers of water-related weather phenomena. It would thus be apt if traces of Dragon-Kings could be found in the atmospheric system. We find no footprints of the legendary creatures in common everyday rainfall but argue for indications of their presence in the form of hurricanes (known as typhoons in the northwestern Pacific), or generally in tropical cyclones. For simplicity, we use the term “hurricane” in the text for strong tropical cyclones in any ocean basin (even when identified by morphology rather than a wind speed criterion), and use the term “tropical cyclone” when we are not referring to the strong-event end of the spectrum. We begin by summarizing a

---

<sup>a</sup> e-mail: ole@santafe.edu

perspective on atmospheric convection and rainfall which we have developed over the past decade and then discuss potential signatures of Dragon-Kings.

Common everyday rain showers come in all sizes, reflected by a broad scaling region in the size distribution. In this region there are no signs of Dragon-Kings, as reviewed below. However, the atmospheric dynamics literature provides evidence that hurricanes are an example of rare extremely large events that result from a switch to a different physical regime [2–5]. Everyday rain showers primarily dissipate energy stored in the atmosphere, whereas hurricanes rely on an efficient way to access warm sea surface water as a different reservoir of energy. Hurricanes are known to be extreme events in different measures – a common definition of a hurricane is a tropical storm with extreme wind speed, for example sustained winds above 74 mph. The high wind speed, a simple threshold, is accompanied by morphological characteristics: the development of a closed-vortex system and the eye in the center. Hurricanes are thus extreme entities, physically different from a convective drizzle, a thunderstorm, a squall line or a large but less-organized mesoscale convective cloud cluster or tropical wave. There is thus reason to postulate a priori, based on the physical differences, that hurricanes may constitute an example of Dragon-Kings in this context. We ask here how they compare in a measure of rain event size.

## 2 Atmospheric convection and rainfall

The rain rate averaged over the globe is about  $0.1 \text{ mmh}^{-1}$ , corresponding to a light drizzle, which also happens to be a common operational definition of detectable *rain* as opposed to *no rain*, for instance with optical rain gauges [6]. Local and highly temporally resolved measurements reveal a great degree of variability. At one-minute and square-decimeter resolution it is not uncommon to observe  $100 \text{ mmh}^{-1}$  in a one-year record in many places on Earth [7]. Taking the resolution to extremes, there is an upper bound on precipitation rates: individual drops cannot fall faster than about 10 m/s, because they become unstable and break up into smaller, slower, droplets at such speeds. This implies an upper bound of about  $10^7 \text{ mmh}^{-1}$  for the rain rate. The durations of rain showers on human scales extend over 7 orders of magnitude from about a millisecond (the impact duration of an individual drop) to several hours in many places. Areas covered by precipitating cloud clusters, again depending on resolution, extend over 18 orders of magnitude from about  $0.1 \text{ mm}^2$  (the size of the smallest individual raindrops [8]) to hundreds of thousands of square-kilometers [9].

This leads to an enormous range of possible event sizes, where an event is defined as the volume of water (proportional to the energy; dimension:  $\text{Length}^3$ ) released from the atmosphere without interruption in space or time on given spatial and temporal resolutions, see Fig. 1.

### 2.1 Event-depth distribution

In 2002, two of us (OP and KC) analyzed a time series from a single location and quantified the event-depth distribution [10]. A time series leaves out the spatial aspect in the sense that space is fixed to the measuring site (one could argue that because the rain field moves across the measuring site, the time series is actually a slice where space and time are mixed). We defined a time event as a sequence of consecutive non-zero rain rates, at one-minute resolution, and the associated event depth as the local depth of the layer of water released,  $d = \sum_{\text{time event}} q(x, y, t) \Delta t$  (dimension: Length), where  $x, y$  are the coordinates of the measuring site and the sum runs over the time

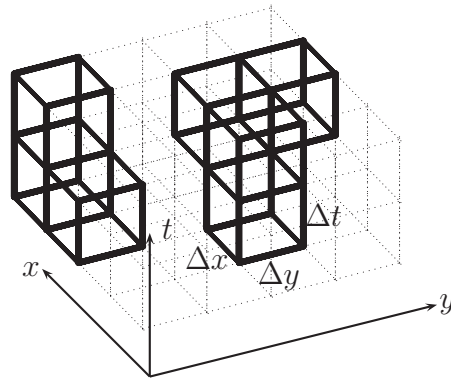


**Fig. 1.** Illustration of the spatio-temporal nature of rain events, where time increases in the up-direction. An event is defined as a cluster of raining nearest neighbors in a discrete space-time (the discreteness being the resolutions of the measurements in space and time), solid lines. Two events are displayed. The event size,  $s$ , is the volume (in  $m^3$ ) of the water released over such a cluster. It is computed by summing the rain rate  $q(x, y, t)$  (dimension: Length/Time) over an event, multiplied by the volume of a voxel in space-time  $\Delta x \Delta y \Delta t$  (dimension:  $\text{Length}^2 \times \text{Time}$ ), that is,  $s = \sum_{\text{event}} q(x, y, t) \Delta x \Delta y \Delta t$  (dimension:  $\text{Length}^3$ ).

event. Similar studies had been attempted earlier with much coarser temporal and rain-rate resolutions [11].

The event depth distribution is very broad [10], and its shape resembles a power law spanning about 3 orders of magnitude, even more in finer resolution. We recently confirmed that power-law exponents fitted to event-depth distributions show little variation between different locations on Earth, provided the measurements are carried out with the same type of instrument at the same resolution [7], see Fig. 2.

The tails of the distributions do not follow an extrapolation of the power law but fall off more rapidly. We interpret this as a reflection of the finite capacity of the system.

There is no evidence of Dragon-Kings in the event-depth distributions, that is, for anomalously high likelihoods of very large events, or a regime shift.

## 2.2 Event-area distribution

Numerous studies have addressed the spatial aspect of rain events in observational work on different types of spatial clusters related to rainfall, clouds and convection [12–21]. We added our own analysis, focusing specifically on the instantaneous area of a precipitation cluster,  $a = \sum_{\text{cluster}} \Delta x \Delta y$  (dimension:  $\text{Length}^2$ ), where the sum runs over a nearest-neighbor cluster of precipitating pixels in one time slice, observed with the precipitation radar on the TRMM (Tropical Rainfall Measuring Mission) satellite [9], using an algorithm from [17], see Fig. 3. Hence, we are not taking into account the rain rates,  $q(x, y, t)$ , nor are we integrating over time.

Similar to the event depths displayed in Fig. 2 [10], the precipitation areas in Fig. 3 [9] have broad distributions, as expected. The distribution resembles a power law over about 3 orders of magnitude for the areas in satellite data.

## 2.3 Self-organized criticality–control & order parameter

The findings of scale-free event-depth and event-area distributions indicate that the system may be an example of self-organized criticality. By this we mean that the

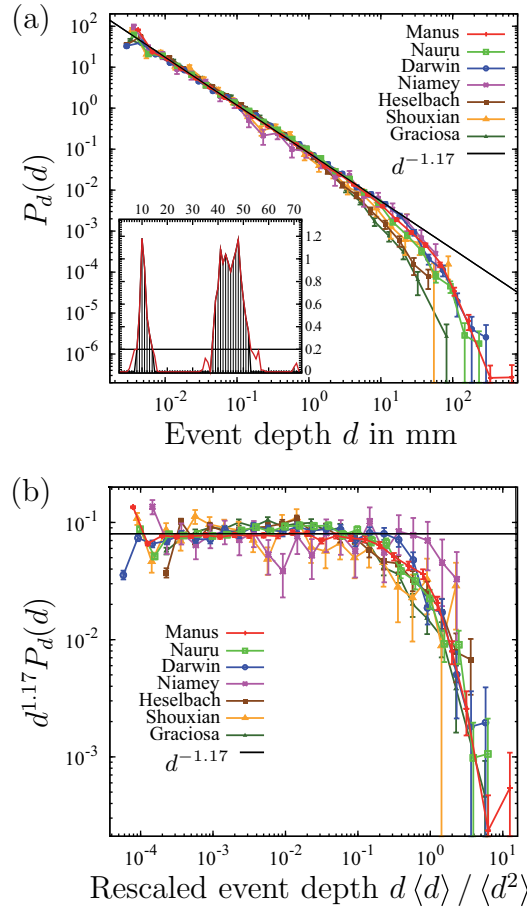


**Fig. 2.** (a) The event-depth probability density function (PDF)  $P_d(d)$  versus event depth  $d$ . Inset: rain-rate *vs.* time, showing two events, defined using the zero-threshold for the measurement (horizontal line). Details in [7]. (b) The transformed PDF,  $d^{\tau_d} P_d(d)$ , where the data in (a) are multiplied with the inverse of the best-fit power law (exponent  $\tau_d = 1.17$ ). The horizontal part, spanning about 3 orders of magnitude, indicates the region where the power law holds, and the upper cutoff, where deviation from the power law becomes significant, is clearly visible.

point at which the atmosphere becomes unstable to convection, or where rainfall is generated, could be the critical point of a continuous phase transition: An order parameter (the rain rate) switches from being zero (*no rain*) to non-zero (*rain*). Moreover, fluctuations in this variable should diverge in the sense that there are spatial and temporal correlations that prevent fluctuations from disappearing with the common dimensional scaling as larger regions of space-time are averaged over. Finally, we expect this critical point to be attractive in the sense that we expect the system to self-organize towards it.

In a 2006 study two of us (OP and DN) tested the hypothesis of such an underlying phase transition more directly [22]. Using satellite estimates [23], we found that averages of the instantaneous precipitation rate,  $q(x, y, t)$ , our supposed order parameter, conditioned on the column-integrated water vapor,  $w(x, y, t)$ , a good proxy for our control parameter, show a sharp power-law-like pick-up above a certain value (the

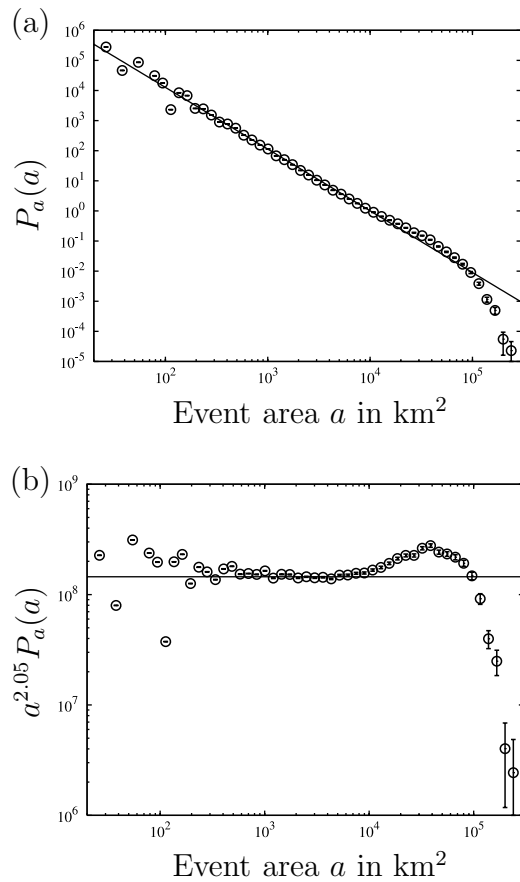


**Fig. 3.** (a) The inferred PDF of cluster areas  $P_a(a)$  versus event area  $a$  (in  $\text{km}^2$ ) in the West Pacific. (b) Transformed PDF,  $a^{2.05} P_a(a)$  versus event area  $a$ . The horizontal line corresponds to a power-law decay of the form  $P_a(a) \propto a^{-2.05}$ . For small areas the discreteness of the lattice becomes important.

“critical point”) of the water vapor, see Fig. 4. This observation,  $\langle q \rangle(w) = a(w - w_c)^\beta$  for  $w > w_c$ , corroborated the hypothesis that the atmospheric system is operating close to a critical point.

Furthermore, the system was mostly found close to the onset of the instability, which we interpreted as evidence for self-organization towards this special point, and we confirmed, using finite-size scaling of the variance of  $q(w)$ , that fluctuations decayed anomalously slowly with averaging scale. These analyses were later improved by including various measures of temperature, both of the sea-surface and of the troposphere [24]. Studies of entire vertical profiles of measures of stability helped explain the success we had had with using only water vapor as a proxy for the control parameter [25].

The idea of an attractive point in the phase space of the atmospheric system that marks the onset of convection was first explicitly communicated by Arakawa and Schubert in 1974 [26], who argued both theoretically and empirically that the troposphere self-organizes to a state, the so-called “Quasi-Equilibrium state” (QE state), where it is marginally convectively stable. Largely, this was thought of as a result of the separation between the fast time scale of convective energy dissipation

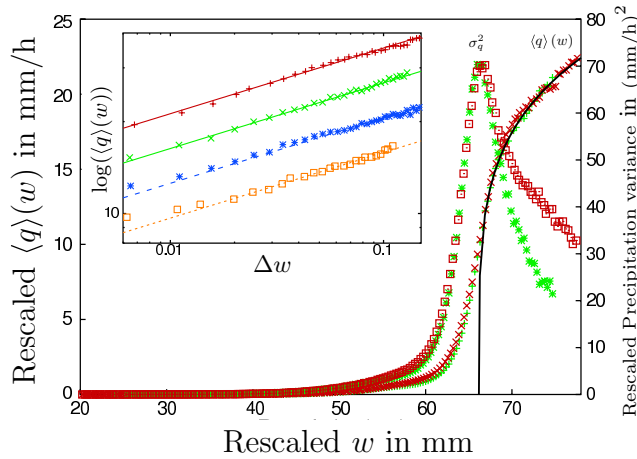


**Fig. 4.** The precipitation rate  $\langle q \rangle(w)$  and its associated variance  $\sigma_q^2$  versus column-integrated water vapor  $w$  for the tropical eastern and western Pacific. The solid line is a fit of the form  $\langle q \rangle(w) = a(w - w_c)^\beta$  for  $w > w_c$  with  $\beta = 0.215$ . The inset displays on double-logarithmic scales the precipitation rate as a function of reduced water vapour  $\Delta w = (w - w_c)/w$  for western Pacific, eastern Pacific, Atlantic, and Indian Ocean (for basin definitions see [22]). The data in the inset are shifted by a small arbitrary factor for visual clarity. The straight lines have slope  $\beta = 0.215$ .

and the slow time scale of destabilization through heating and moistening near the ground and radiative cooling aloft.

Thus our own studies – re-phrased in our current understanding of the problem – are consistent with the hypothesis that the QE state may be critical.

### 3 Dragon-Kings

We have shown above that the distributions of event-depth (dimension: Length) and event-area (dimension: Length<sup>2</sup>) are very broad, see Fig. 2 and Fig. 3. We were not able to measure exactly what we would like to measure, namely the size  $s = \sum_{\text{event}} q(x, y, t) \Delta x \Delta y \Delta t$  (dimension: Length<sup>3</sup>), where the sum runs over the event, because data sets that cover both time and space at acceptable resolutions are difficult to construct. If such data were available, a new feature might emerge. Whereas the distributions displayed in Fig. 2 and Fig. 3 seemed to cut off sharply beyond a certain scale, it seems likely that in the fully space-time integrated sense hurricanes constitute a different kind of event. Hurricanes are effective heat engines that connect the atmospheric surface boundary layer (which is warmed and moistened by ocean surface water) to the cold tropopause. Strong surface winds enhance the transfer of energy from the sea surface [2]. Other precipitating systems with specific relations of wind speed and moist convection can be sustained by similar mechanisms [27, 28], but the strong winds permitted by the closed vortex morphology of hurricanes contribute to much more effective maintenance of the system. These heat engines can sustain themselves over many days or even weeks, underscoring the differences from ordinary cloud clusters, which tend to fall apart more rapidly.

In a previous study, two of us (OP and DN) investigated the relationship in Fig. 4 using pixels from a space-time window that included Hurricane Katrina [29], see Fig. 5. The conditioned precipitation rate picks up similarly as a function of

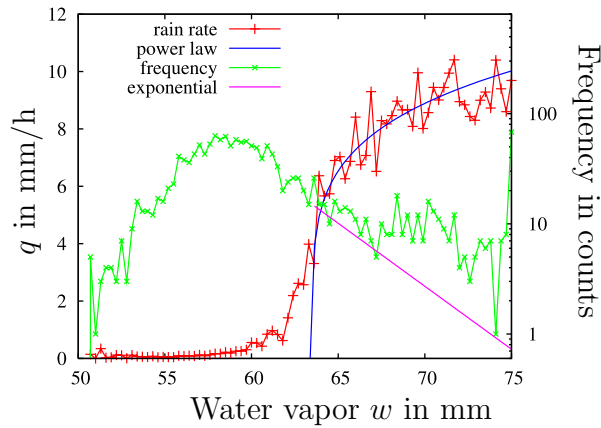


**Fig. 5.** The rain rate versus the water vapor from TRMM microwave retrievals during hurricane Katrina (red symbols). Note the similarity with the data displayed in Fig. 4. Indeed, the blue line is a fit of the form  $(w - w_c)^\beta$  with  $\beta = 0.21$ . The difference in estimates of the rain rate amplitude is due to an updated retrieval algorithm being used here [30], and the difference in  $w_c$  reflects the difference in tropospheric temperatures in the West Pacific and the Gulf of Mexico. The green symbols show the frequency at which a given water vapor was observed (precipitating pixels only, logarithmic right  $y$ -axis), and the turquoise straight line represents an exponential decay as is observed in less organized convection [29], which we claim does not fit to the hurricane data.

water vapor. But the frequency with which high water vapor occurred is different (green line in Fig. 5). In [24] the frequency of water vapor in precipitating pixels was found to be approximately symmetric about the maximum just below  $w_c$  and to decay approximately exponentially above  $w_c$  at a rate of  $3.8 \text{ mm}^{-1}$ , represented by the turquoise line in Fig. 5. While the sample is small, neither is this line a good fit to the hurricane data, nor does the distribution (green line) look symmetric. The hurricane sustained over a period of several days a level of water vapor that usually only occurs very rarely and for brief periods, resulting in relatively many high-water vapor measurements. The value of 75 mm was reached 68 times (green symbols in Fig. 5). This bin appears to include measurements that maxed out the retrieval algorithm.

This is the signature of the fundamentally different dynamics by which high values of water vapor are maintained over a long time within hurricanes. In order to quantify this in observations we looked for time series that contained data collected during a hurricane. The only series we found was from an ongoing experiment in Barbados, carried out by the Max-Planck Institute for Meteorology in Hamburg. On 29 October 2010, the measuring site was hit by hurricane Tomas. Unfortunately, the hurricane led to a loss of electricity on the island and the time series was interrupted. We mention this here to make a point about extreme events: Truly extreme events that result from different physical processes and may be orders of magnitude smaller or larger than “ordinary” events may often be missed because they escape our attention, measurements are not designed to capture them, or people have other things to worry about than academic interests.

### 3.1 Event power

Using the precipitation clusters defined in [9], we make another attempt at identifying the nature of the largest spatio-temporally integrated rain events. Instead

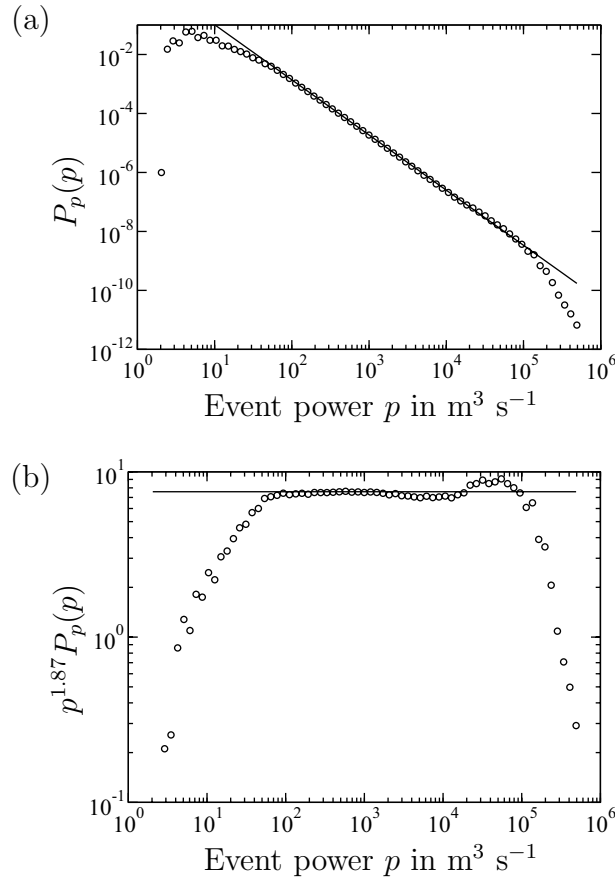


**Fig. 6.** (a) The inferred PDF of event power  $P_p(p)$  versus event power  $p$  (in  $\text{m}^3\text{s}^{-1}$ ) in the West Pacific from 1 January 1998 till 31 December 2006 (open circles) from TRMM radar retrievals, see [9]. The straight line has slope  $-1.87$ . (b) Transformed PDF,  $p^{1.87}P_p(p)$  versus event power  $p$ . Hence, a horizontal line corresponds to a power-law decay of the form  $P_p(p) \propto p^{-1.87}$ .

of focusing on the depth or the area of a precipitation cluster, we compute the total instantaneous precipitation rate in a cluster, which we call the event power,  $p = \sum_{\text{cluster}} q(x, y, t) \Delta x \Delta y$  (dimension:  $\text{Length}^3/\text{Time}$ ), where the sum, like for the areas, runs over a cluster of nearest-neighbor precipitating pixels in a single time slice. This yields the volume of water per time that is shed from the cluster. It misses the time dimension in that it does not contain any information about how long the cluster continued to shed water at this rate. We expect hurricanes to be large in this measure, even though it does not include their distinguishing persistence.

The event power PDF is shown in Fig. 6. Similar to the event depth and event area, the event power has a broad distribution. We find that the data is consistent with a power-law decay over approximately 3 orders of magnitude.

Next, we identified the 10 most powerful clusters for each ocean basin and inspected them in satellite microwave retrievals [30] (available from [http://www.ssmi.com/tmi/tmi\\_daily.html](http://www.ssmi.com/tmi/tmi_daily.html)), to check which were tropical cyclones. We did this by eye based on morphological characteristics and persistence, using data for precipitation, water vapor and wind. Each cluster was located in the satellite image, and we looked



for approximately circular structure in the rain field (aside from the characteristic rain bands that break circular symmetry), examining also images from 2 days before and after the event to clarify whether not fully closed vortices would eventually turn into, or were the remnants of, tropical cyclones, using persistence of the circular structure as another criterion for classification. The border-line cases would have been classified either as hurricanes or as tropical storms in named-hurricane lists. The choice of these criteria was made to avoid using an explicit amplitude threshold in the definition, as is the case for “named storm” criteria (which use wind speed thresholds in determining when a tropical storm is assigned a name and when it enters the hurricane category).

Out of the 10 most powerful clusters, one was a hurricane in the Atlantic basin, where the largest systems tend to be convective clusters in the Gulf of Guinea; none in the East Pacific, where the largest systems are far off the (cold-water) American West coast towards the West Pacific; two were hurricane-like tropical storms in the Indian Ocean, and 7 out of 10 were hurricanes or hurricane-like in the West Pacific. In the West Pacific there is one instance in the 10 most powerful events of a hurricane being counted twice, during different overpasses of the satellite – the 3rd and 4th largest events here are the same hurricane (on 13 April 2004), illustrating the persistence argument. No non-hurricanes appeared twice in this list.

We then focused on the West Pacific and looked at the 400 most powerful events, categorizing them as hurricanes or non-hurricanes, again by eye as described above. We identified a total of 87 hurricanes and 313 non-hurricanes.

We compared these results to the following automated procedure: we used the Best Track Archive for named storms of the Joint Typhoon Warning Center, available at <http://www.usno.navy.mil/JTWC/>. Clusters were identified as hurricanes if they were within two days and  $\pm 10^\circ$  of the track of a named storm in the typhoon or supertyphoon category. We found close correspondence between hurricanes identified by eye and automatically, and continued to use the automated procedure for the largest 10,000 clusters in West Pacific.

Figure 7(a) displays these 10,000 events in ranked order, that is, the most powerful event is given rank 1, the next-largest event is given rank 2 and so on. The approximately exponential range in this figure (from about  $100,000 \text{ m}^3\text{s}^{-1}$  corresponds roughly to the region in Fig. 6 above the large-scale cutoff, where the power law breaks down. Also shown are the ranked hurricanes (red circles with line), where the largest hurricane is assigned rank 1, the second-largest hurricane rank 2 *etc.*, and the ranked non-hurricanes (black squares with line). In Fig. 7(b) we show the fraction of events larger than a given size that are hurricanes. This fraction increases with event power, showing that the extreme tail is dominated by hurricanes. If we restrict the analysis to geographic regions and seasons known to be physically most favorable to hurricane formation, more non-hurricanes than hurricanes are eliminated, and the transition from the non-hurricane to hurricane regime changes slightly, but the general picture remains similar (not shown).

Figure 7(b) conveys an impression of statistical significance. Our observations suggest that the tail of the distribution is dominated by hurricanes. The figure shows an increase with size in the proportion of observed events larger than a given size being hurricanes. But since the number of observations decreases towards the extreme tail of the distribution, the significance of this observation decreases here too. By significance we mean here a likelihood that in some ensemble of similar observations a similar trend would be observed. For a rough quantitative estimate of that likelihood we assume the following null model (to generate a reference ensemble): events are either hurricanes or not, with probability  $738/9,967 \approx 7.40\%$ , i.e. the proportion of hurricanes in all observed events equally sized or larger than the smallest observed hurricane, such that the number of hurricanes in any sub-set of events is binomially distributed.

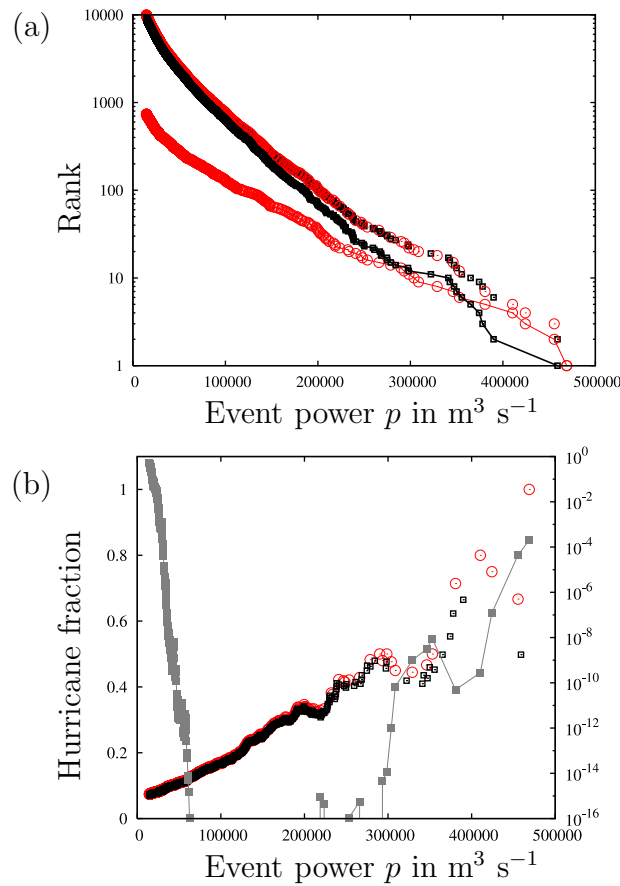


**Fig. 7.** (a) Rank (see text) of events, hurricanes and non-hurricanes as a function of event power, focusing on the tail of the event-power PDF from Fig. 6, displaying the 10,000 largest events (symbols only), the 738 largest hurricanes (red circles with lines), and the largest 9,262 non-hurricanes (black circles with line), indicating that even without taking the duration of the events into account, the hurricanes dominate the tail. The  $y$ -axis is logarithmic so that a straight line corresponds to an exponential decay. (b) For each event in the tail, whether hurricane (red circle) or not (black square) we show the fraction of events larger than  $p$  that are hurricanes. The solid black squares (with line) indicate the likelihood (see main text) for an equal or greater number of hurricanes to be observed in the sample of events larger than  $p$ . The null model forces this likelihood to be  $1/2$  at the lower end, values are shown on the right vertical axis. Even in the extreme tail, where the statistics are worse, the likelihood of obtaining the observations from the null model (see text) is smaller than one in a thousand.

What then would be the probability to observe an equal or greater proportion of hurricanes than was actually observed, as a function of event size? This probability is shown on the right-hand vertical axis in Fig. 7(b), using the Gaussian approximation to the binomial distribution. By construction, this likelihood is  $1/2$  for the smallest hurricane. It initially decays quickly to below  $10^{-16}$  and increases again in the extreme tail, where the statistics worsen, to a maximum for the largest hurricane of less than  $10^{-3}$ . In other words, even where the statistics are worse, less than one in a thousand ensemble members (based on the null model) will produce a hurricane propensity equal to or larger than the observations.

Whether hurricanes are Dragon-Kings in the sense of generating more-likely extreme events than a simple extrapolation of the body of the distribution would suggest, as proposed in Ref. [1], depends on the distribution that is being extrapolated. Where the power law holds, hurricanes are statistically insignificant in number. Beyond the cutoff, for  $p > 10^5 \text{ m}^3\text{s}^{-1}$ , say, one could be tempted to approximate the distribution by an exponential or some other fast-decaying function. Without a separate criterion to distinguish among events, the fit of such a function to data would be heavily influenced by hurricanes. Because we have available separate criteria to distinguish hurricanes, it may be seen (Figure 7a) that the contribution to the tail associated with them falls much less quickly than that associated with other events. It is thus reasonable to use the term Dragon-Kings for hurricanes to refer to the fact that they are extreme in this measure and different from other events in morphology and longevity.

Corral, Osso and Llebot [31] followed named storms through space and time, which enabled them to observe something similar to the energy released in space-time events of the type illustrated in Fig. 1. They found that estimates of the energy dissipated through surface drag in a hurricane over its lifetime ranged over about two orders of magnitude in a broad power-law like distribution. Our measure of hurricane size does not allow us to test this observation. Firstly because we can only look at the very large-event tail of the distribution (smaller observed power may be the result of a hurricane lying only partly inside the satellite swath), secondly because we use a measure of energy dissipated per time, whereas Ref. [31] estimated total energy dissipated, *i.e.*, integrated over time. This integration necessarily broadens the distribution. Our data do not allow a similar integration. It is instructive to compare different estimates of event power. Measures of energy dissipated by surface drag in the atmospheric boundary layer are relevant to the destructive power of storms. Emanuel estimates this power of a large Pacific supertyphoon as  $3 \times 10^{13} \text{ W}$  [32]. Our measure in  $\text{m}^3 \text{ s}^{-1}$  can be converted into Watts using the latent heat of water. This procedure yields an estimate of the total power generated by the hurricane heat engine. This is considerably larger than the power dissipated through surface drag because much of the energy goes into the increase in potential energy of air lifted in the storm (which descends over large distances). Figure 7 ranges up to powers of  $10^{15} \text{ W}$ , in agreement with other estimates of the same quantity [33] for the largest typhoons, and a good order of magnitude more than Emanuel's estimate for the maximum surface-drag energy dissipation rate.

### 3.2 Summary

Asking whether, in the context of rainfall, "Dragon-Kings" can be thought of as exemplified by hurricanes, we find that the answer requires one to define what appears to be a borderline case. On the one hand, hurricanes are extreme events that rely on physical processes which are different from those at work in everyday events. Even for large available data sets, it is challenging to quantify in how far the hurricanes dominate the tail of event size distributions because measurements of extremes are rare, technically difficult, and the measure in which we expect rainfall from hurricanes to be most distinct cannot be obtained because of a lack of spatio-temporally complete highly resolved data sets. Ordinary precipitation events exhibit a power-law distribution in a measure of their size (event power, *i.e.*, rain rate integrated spatially over an event). If the definition of Dragon-Kings is taken to be restricted to phenomena that stand distinctly above the power law in the size distribution, then hurricanes do not fall into this category. Nonetheless, we find evidence that hurricanes extend the tail in a manner that greatly increases the probability of the largest event sizes.

This occurs where the distribution of non-hurricane events reaches the roughly exponential cut off at the end of the power law range. As a distinct physical process that generates extreme events beyond the distribution of ordinary events hurricanes are, if not Dragon-Kings, at least Dragon Princes.

We would like to thank L. Nuijens for processing micro rain radar data from the Barbados site and making them available to us in near-real time. Cluster data for Fig. 3 and Fig. 6 were generated by S. Nesbitt for Ref. [9]. A. Deluca and A. Corral helped compile and analyze data shown in Fig. 2 for Ref. [7]. O.P. acknowledges support from ZONlab ltd. D.N. acknowledges support from National Science Foundation AGS-1102838.

## References

1. D. Sornette, *Int. J. Terraspace Sci. Eng.* **2**, 1 (2009), <http://arXiv.org/abs/0907.4290>
2. K.A. Emanuel, *J. Atmos. Sci.* **43**, 585 (1986)
3. R.A. Houze, *Cloud Dynamics* (Academic Press, 1993)
4. G.J. Holland, *J. Atmos. Sci.* **54**, 2519 (1997)
5. K.A. Emanuel, C. DesAutels, C. Holloway, R. Korty, *J. Atmos. Sci.* **61**, 843 (2004)
6. G.M. Stokes, S.E. Schwartz, *Bull. Amer. Meteor. Soc.* **75**, 1201 (1994)
7. O. Peters, A. Deluca, A. Corral, J.D. Neelin, C.E. Holloway, *J. Stat. Mech.* P11030 (2010)
8. R.R. Rogers, M.K. Yau, *A short course in cloud physics*, 3rd edn. (Butterworth-Heinemann, 1989)
9. O. Peters, J.D. Neelin, S. Nesbitt, *J. Atmos. Sci.* **66**, 2913 (2009)
10. H. Peters, C. Hertlein, K. Christensen, *Phys. Rev. Lett.* **88**, 018701 (2002)
11. R.F.S. Andrade, H.J. Schellnhuber, M. Claussen, *Physica A* **254**, 557 (1998)
12. R.A. López, *Mon. Wea. Rev.* **105**, 865 (1977)
13. R.A.J. Houze, C.-P. Cheng, *Mon. Wea. Rev.* **105**, 964 (1977)
14. M. Williams, R.A.J. Houze, *Mon. Wea. Rev.* **115**, 505 (1987)
15. R.A.J. Houze, *Cloud Dynamics* (Academic Press Inc, San Diego, 1993b)
16. B.E. Mapes, R.A.J. Houze, *Mon. Wea. Rev.* **121**, 1398 (1993)
17. S. Nesbitt, W.R. Cifelli, S.A. Rutledge, *Mon. Wea. Rev.* **134**, 2702 (2006)
18. R.F. Cahalan, J.H. Joseph, *Mon. Wea. Rev.* **117**, 261 (1989)
19. T.C. Benner, J.A. Curry, *J. Geophys. Res.* **103**, 28753 (1998)
20. R.A.J. Neggers, H.J.J. Jonker, A.P. Siebesma, *J. Atmos. Sci.* **60**, 1060 (2003)
21. R.A.J. Houze, C.-P. Cheng, *Mon. Wea. Rev.* **107**, 1370 (1979)
22. O. Peters, J.D. Neelin, *Nature Phys.* **2**, 393 (2006)
23. F.J. Wentz, R.W. Spencer, *J. Atmos. Sci.* **55**, 1613 (1998)
24. J.D. Neelin, O. Peters, K. Hales, *J. Atmos. Sci.* **66**, 2367 (2009)
25. C.E. Holloway, J.D. Neelin, *J. Atmos. Sci.* **66**, 1665 (2009)
26. A. Arakawa, W.H. Schubert, *J. Atmos. Sci.* **31**, 674 (1974)
27. J.D. Neelin, I.M. Held, K.H. Cook, *J. Atmos. Sci.* **44**, 2341 (1987)
28. C.S. Bretherton, P.N. Blossey, M. Khairoutdinov, *J. Atmos. Sci.* **62**, 4273 (2005)
29. O. Peters, D. Neelin, *Int. J. Mod. Phys. B* **23**, 5453 (2009)
30. K.A. Hilburn, F.J. Wentz, *J. Appl. Meteor. Clim.* **47**, 778 (2008)
31. Álvaro Corral, A. Ossó, J.E. Llebot, *Nature Phys.* **6**, 693 (2010)
32. K.A. Emanuel, *Weather* **54**, 107 (1999)
33. R.A. Anthes, H.A. Panofsky, J. Cahir, A. Rango, *The atmosphere*, 2nd edn. (Charles E. Merrill, Columbus Ohio, 1978)